Inorganic Chemistry

Article

pubs.acs.org/IC

Stable Plumbylene Dichalcogenolate Monomers with Large Differences in Their Interligand Angles and the Synthesis and Characterization of a Monothiolato Pb(II) Bromide and Lithium Trithiolato Plumbate

Brian D. Rekken, Thomas M. Brown,† Marilyn M. Olmstead, James C. Fettinger, and Philip P. Power*

Department of Chemistry, University of California—Davis, Davis, California 95616, United States

Supporting Information

ABSTRACT: The complexes, $Pb(ChAr^{Pri_4})_2$ (Ch = O (**1**), S (**2**); Ar^{Pri_4} = C_6H_3-2,6-(C_6H_3-2,6-Pr^i_2)$_2$) were synthesized by alcoholysis and salt metathesis routes and represent the first fully characterized monomeric, two-coordinate, lead dichalcogenolates in the solid state. Structural studies showed that the S−Pb−S angle (77.21(4)°) is about 22° narrower than the corresponding O−Pb−O angle. ^{207}Pb NMR and electronic spectroscopy show that the separation between the highest occupied molecular orbital (HOMO) and the lowest unoccupied molecular orbital (LUMO) decreases from the bisaryloxo plumbylene to the bisthiolato derivative. Reaction of $LiSAr^{Me_6}$ with $PbBr_2$ in a 2:1 ratio led not to $Pb(SAr^{Me_6})_2$, but to a mixture of the monothiolato lead(II) complex, {Pb(Br)(μ-SAr^{Me_6})}$_2$ (**3**) and the lithium tristhiolato plumbate, $LiPb(SAr^{Me_6})_3$ (**4**). **3** and **4** were isolated and purified by fractional recrystallization, and both were characterized by X-ray crystallography and spectroscopic studies.

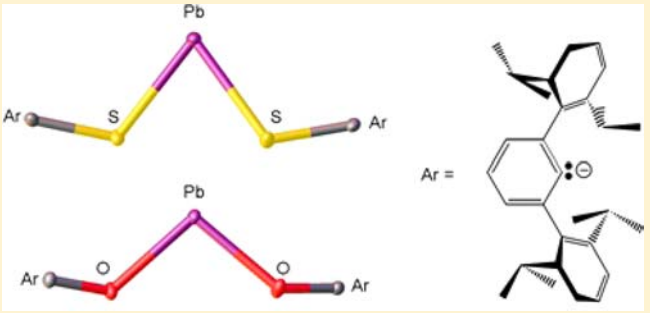

INTRODUCTION

Plumbylenes are the heaviest analogues of carbenes.[1] Unlike carbon, the lead 2+ oxidation state is favored over lead 4+ in their inorganic derivatives because of the increasing stabilization of the s-valence electrons.[2] Nonetheless, the isolation of stable monomeric, two-coordinate plumbylenes has proven more difficult than their lighter group 14 congeners because of their greater sensitivity to heat and light.[3] The first stable diorganoplumbylene, $Pb\{CH(SiMe_3)_2\}_2$, was reported by Lappert et al in 1973.[4] Although it is a monomer in solution, its crystal structure was not obtained until 1998 by Klinkhammer which revealed the plumbylene to be a weakly associated dimer featuring a long Pb−Pb bond of 4.129 Å.[5] The isoelectronic $-N(SiMe_3)_2$, substituted amido derivative, was prepared in 1974;[6] and the structure of $Pb\{N(SiMe_3)_2\}_2$ was determined in 1983 where it was shown to be a two-coordinate, V-shaped monomer.[7] For chalcogenolates, homoleptic lead(II) dichalcogenolate derivatives, $Pb(BHT)_2$[8] and $Pb(SMes^*)_2$[9] (BHTH = butylated hydroxytoluene, HOC_6H_2-2,6-Bu^t_2-4-Me; Mes* = C_6H_2-2,4,6-Bu^t_3) were prepared in 1980 and 1983, respectively. The former species was reported in a review to be a monomer based upon weak X-ray data while the structure of $Pb(SMes^*)_2$ currently remains unknown.[10] The structure of the related bisthiolato plumbylene, $Pb(SC_6H_3$-2,6-$Pr^i_2)_2$ was determined to be a trimer in the solid-state.[10] Subsequently, several sterically encumbered bisthiolato derivatives of Pb(II, including $[Pb\{SC(SiMe_3)_3\}\{\mu$-$SC(SiMe_3)_3\}]_2$[11] and $[Pb\{SSi(OBu^t)_3\}\{\mu$-$SSi(OBu^t)_3\}]_2$, have been isolated. Despite the large size of their thiolate substituents, they are dimeric and feature a four-member Pb_2S_2 ring with three-coordinate lead atoms[12] Currently, the only fully structurally characterized, two-coordinate plumbylene featuring a Pb−chalcogen bond is the heteroleptic, aryl−arylthiolato species, Pb(Tbt)(STbt) (Tbt = C_6H_2-2,4,6-$\{CH(SiMe_3)_2\}_3$), which was obtained by Okazaki, Tokitoh, and co-workers via a 1,2 aryl migration from the corresponding plumbanethione, $(Tbt)_2PbS$.[13]

The development and understanding of the bonding in two-coordinate, lead dichalcogenolates is marked by the fact that all fully characterized examples are either polymers, oligomers, or base-stabilized adducts in the solid-state.[14] Such species could be of practical importance as precursors for important semiconductors, such as PbS,[15] and complexes of general formula, $[Pb(OR)_2]_n$ have proven useful in the preparation of the piezoelectric ceramic, PZT, found in numerous electromechanical applications such as ultrasound generators and sonar detectors.[16] The aryloxide, $Pb(OC_6H_3$-2,6-$Bu^t_2)_2$, (structure unknown) has been used to synthesize the three-coordinate lead(II) complex, $Pb(OC_6H_3$-2,6-$Bu^t_2)\{N(C_6H_3$-2,6-$Pr^i_2)C(CH_3)\}_2CH$, in which the aryloxide ligand functions as a pseudohalide and was shown to be resistant to decomposition in contrast to the corresponding halide

Received: November 16, 2012
Published: February 26, 2013

dx.doi.org/10.1021/ic302513c | Inorg. Chem. 2013, 52, 3054−3062

derivatives.[17] Subsequent reactions established that the remaining aryloxide ligand could be replaced by the amido ($-N(SiMe_3)_2$), phosphido ($-P(SiMe_3)_2$), or P-phosphasileno ($-P{=}Si(R)Si(Bu^t)_3$, R = C_6H_2-2,4,6-Pr^i_3) functional groups.[17] Furthermore, variations of this complex demonstrated reversible reactivity with carbon dioxide that may lead to new methods for CO_2 sequestration purposes.[18] Bisthiolato plumbylenes may also prove to have relevance for the interaction of lead with disulfide bridges in cases of lead poisonings.[19] Where anemia-related symptoms for such poisonings have been, studies have shown that the lead(II) atom embeds itself into the zinc enzyme, aminolevulinic acid dehydratase (ALAD),[19,20] which possesses a trigonal pyramidal Zn(II)(cystine)$_3$ site (atypical geometry for zinc),[19,21] for which lead has a 500 times greater affinity.[22] However, fine details regarding the exact geometry of the trithiolato lead(II) site remain ambiguous, and the number of model compounds is limited.[22−25] We now report the synthesis and characterization of the monomeric two-coordinate plumbylene dichalcogenolates, the isolobal $Pb(OAr^{Pri_4})_2$, (**1**), and $Pb(SAr^{Pri_4})_2$, (**2**); Ar^{Pri_4} = C_6H_3-2,6(C_6H_3-2,6-Pr^i_2)$_2$) which are stabilized by bulky chalcogenolate ligands that carry the same terphenyl substituent but feature Ch−Pb−Ch angles that differ by about 22°. In addition, the monothiolato lead(II) bromide, {Pb(μ-SAr^{Me_6})Br}$_2$ (**3**), and the lithium tristhiolato lead(II) complex, LiPb(μ-SAr^{Me_6})$_3$ (**4**) were isolated during attempts to synthesize the less sterically crowded lead dithiolate, $Pb(SAr^{Me_6})_2$.

EXPERIMENTAL SECTION

All manipulations were performed with the use of modified Schlenk techniques under an N_2 atmosphere or in a Vacuum Atmospheres drybox under N_2. Solvents were distilled over a potassium mirror and degassed immediately prior to use via freeze−pump−thaw cycles. Unless otherwise noted, all chemicals were obtained from commercial sources and used without further purification. $HOAr^{Pri_4}$, $HSAr^{Pri_4}$, $HSAr^{Me_6}$ $LiOAr^{Pri_4}$,[27a] $LiSAr^{Me_6}$,[26] $LiSAr^{Pri_4}$,[27b] and $Pb\{N(SiMe_3)_2\}_2$[6] were prepared according to literature procedures.[26,27] ^1H and ^{13}C NMR spectra were recorded on a Varian 600 MHz instrument and referenced internally to either protio benzene or trace silicone grease (δ = 0.29 in C_6D_6). ^{207}Pb NMR (operating at 125.53 MHz) spectra were acquired on a Varian 600 MHz instrument and were referenced to $PbMe_4$ in C_6D_6 (δ = 0). IR spectra were recorded as Nujol mulls between CsI plates on a Perkin-Elmer 1430 spectrophotometer. UV−visible spectra were recorded as dilute hexanes solutions in 3.5 mL quartz cuvettes using a HP 8452 diode-array spectrophotometer. Melting points were determined on a Meltemp II apparatus using glass capillaries sealed with vacuum grease and are uncorrected.

$Pb(OAr^{Pri_4})_2$ (1). A solution of 0.951 g (2.30 mmol) of $HOAr^{Pri_4}$ dissolved in diethyl ether (45 mL) and cooled to about 0 °C was added over 20 min to a diethyl ether solution (10 mL) of 0.548 g (1.15 mmol) of $Pb\{N(SiMe_3)_2\}_2$ cooled to 0 °C wrapped in aluminum foil. The solution was stirred for 1 h and then allowed to warm to ambient temperatures and was stirred for an additional 8 h to give a clear, pale yellow solution. The solution was concentrated to about 5 mL and cooled to about 6 °C for 2 days to produce X-ray quality, pale yellow crystalline blocks of **1** as a solvate with 0.5 molecules of diethyl ether. A small amount of lead metal was also deposited. Yield: 0.664 g (0.640 mmol, 56%) mp: 295 °C. ^1H NMR (599.7 MHz, C_6D_6, 303 K): δ = 1.07 (d, 24H, $CH(CH_3)_2$, $^3J_{HH}$ = 7.20 Hz), 1.09 (d, 24H, $CH(CH_3)_2$, $^3J_{HH}$ = 6.60 Hz), 2.97 (m, 8H, $CH(CH_3)_2$, $^3J_{HH}$ = 6.60 Hz), 6.72 (t, 2H, p-C_6H_3, $^3J_{HH}$ = 6.90 Hz), 7.08 (d, 4H, m-C_6H_3, $^3J_{HH}$ = 7.05 Hz), 7.19 (d, 8H, m-$C_6H_3iPr_2$, $^3J_{HH}$ = 7.04 Hz), 7.21 (t, 4H, p-$C_6H_3iPr_2$, $^3J_{HH}$ = 7.04 Hz); $^{13}C\{^1H\}$ NMR (150.8 MHz, C_6D_6, 296 K): δ = 23.87 (o-$CH(CH_3)_2$), 24.86 (o-$CH(CH_3)_2$), 30.75 (o-$CH(CH_3)_2$), 116.24, (m-$C_6H_2iPr_3$), 124.47 (p-C_6H_3), 128.60 (m-C_6H_3), 130.56 (o-C_6H_3), 130.64 (p-$C_6H_2iPr_2$), 140.06 (o-$C_6H_2iPr_2$), 148.36 (i-$C_6H_2iPr_2$), 161.53 (i-C_6H_3); $^{207}Pb\{^1H\}$NMR (125.53 MHz, C_6D_6, 296 K): δ = 1070.3; UV−vis: [λ, nm (ε, M^{-1} cm^{-1})] 370 (850), 300 (2950), 293 (3200). IR (cm^{-1}): (Pb−O) 490.

$Pb(SAr^{Pri_4})_2$ (2). A slurry of $LiSAr^{Pri_4}$ (1.266 g, 2.90 mmol) in diethyl ether (60 mL) was added dropwise over 45 min to a diethyl ether slurry (10 mL) of $PbBr_2$ (0.532 g, 1.45 mmol) cooled in an ice bath. The solution became yellow immediately and, after 1 h, the solution was allowed to warm to ambient temperature and was stirred overnight to give an orange solution. All volatile components were removed under reduced pressure, and the residue was extracted with toluene (60 mL) and filtered. The solution was concentrated to about 20 mL, and cooled overnight to about 6 °C to give **2** as a microcrystalline, yellow powder. The solution was further concentrated to about 5 mL to give a second crop of the crystals. The supernatant liquid was decanted, and a small amount of **2** (ca. 0.04 g) was dissolved in a concentrated tetrahydrofuran (THF) solution and stored at −17 °C for 4 days to yield X-ray quality, yellow crystals of **2** as a solvate with 2 THF molecules. Yield: 0.643 g (0.620 mmol, 43%). mp 211−214 °C; ^1H NMR (599.7 MHz, C_6D_6, 294 K): δ = 1.07 (d, 24H, $CH(CH_3)_2$, $^3J_{HH}$ = 6.60 Hz), 1.23 (d, 24H, $CH(CH_3)_2$, $^3J_{HH}$ = 7.20 Hz), 2.84 (m, 8H, $CH(CH)_2$, $^3J_{HH}$ = 6.60 Hz), 6.85 (t, 4H, p-$C_6H_3iPr_2$, $^3J_{HH}$ = 7.20 Hz), 7.06 (d, 8H, m-$C_6H_3iPr_2$, $^3J_{HH}$ = 7.80 Hz), 7.15 (t, 2H, p-C_6H_3, $^3J_{HH}$ = 6.20 Hz), 7.16 (d, 4H, m-C_6H_3, $^3J_{HH}$ = 5.40 Hz); $^{13}C\{^1H\}$ NMR (150.8 MHz, C_6D_6, 296 K): δ = 24.09 (o-$CH(CH_3)_2$), 24.94 (o-$CH(CH_3)_2$), 31.05 (o-$CH(CH_3)_2$), 123.40 (m-$C_6H_2iPr_3$), 123.98 (p-C_6H_3), 128.59 (m-C_6H_3), 129.26 (o-C_6H_3), 140.70 (p-$C_6H_2iPr_2$), 141.68 (o-$C_6H_2iPr_2$), 144.32 (i-$C_6H_2iPr_2$), 147.45 (i-C_6H_3); $^{207}Pb\{^1H\}$NMR (125.53 MHz, C_6D_6, 296 K): δ = 4283. UV−vis: [λ, nm (ε, M^{-1} cm^{-1})] 422 (1300), 354 (1100), 292 (5800). IR: The Pb−S stretching band is tentatively assigned to an absorption at 302 cm^{-1}.

{Pb(μ-SAr^{Me_6})Br}$_2$ (3) and LiPb(μ-SAr^{Me_6})$_3$ (4). $LiSAr^{Me_6}$ (1.282 g, 3.64 mmol) was dissolved in about 60 mL of diethyl ether and added dropwise over 30 min to a diethyl ether (10 mL) slurry of $PbBr_2$ (0.668 g, 1.82 mmol) cooled to about −78 °C. After addition, the solution was stirred at about −78 °C for a further 1 h and then allowed to warm slowly to room temperature. The solution was stirred for 2 d to give a pale yellow solution and a white precipitate. All the volatile components were removed under reduced pressure. Toluene (80 mL) was added, and filtration afforded a clear, faint yellow solution. The filtrate was concentrated under reduced pressure to about 60 mL and placed in an about −17 °C freezer to afford X-ray quality crystals of **4** as colorless blocks after 3 days (0.732 g). The supernatant liquid was decanted, and concentrated to about 30 mL and placed in an about −17 freezer to afford a second fraction of **4** (0.369 g) after 2 days. The supernatant liquid was decanted, and concentrated to about 15 mL and placed in an about −17 °C freezer to afford X-ray quality crystals of **3** as colorless prisms after 4 days (0.387 g). The supernatant liquid was decanted into a second flask, and concentrated to about 8 mL and placed in an about −17 °C freezer to afford a second fraction of **3** (0.114 g) after 5 days. Attempts to isolate any further fractions were unsuccessful. The total yield of {Pb(μ-SAr^{Me_6})Br}$_2$ (**3**): 0.501 g (0.382 mmol, 42.0%) mp 268−270 °C. ^1H NMR (599.7 MHz, C_6D_6, 294 K): δ = 2.20 (s, 24H, o-CH_3), 2.27 (s, 12H, p-CH_3), 6.82 (s, 8H, $C_6H_2Me_3$), 6.84 (d, 4H, m-C_6H_3, $^3J_{H,H}$ = 7.34 Hz), 7.13 (t, 2H, p-C_6H_3, $^3J_{H,H}$ = 7.34 Hz); $^{13}C\{^1H\}$ NMR (C_6D_6, 150.8 MHz, 296 K): δ = 21.56 (p-CH_3), 21.69 (o-CH_3), 125.75 (p-C_6H_3), 129.69 (o-$C_6H_2Me_3$), 130.08 (m-C_6H_3), 135.27 (o-C_6H_3), 137.84 (m-$C_6H_2Me_3$), 138.26 (p-$C_6H_2Me_3$), 138.91 (i-$C_6H_2Me_3$), 144.37 (i-C_6H_3); ^{207}Pb NMR (125.5 MHz, C_6D_6, 296 K): δ = 2223.0 ppm; IR: The Pb−S stretching band is tentatively assigned to an absorption at 340 cm^{-1}. Total yield of LiPb(μ-SAr^{Me_6})$_3$ (**4**): 1.101 g (0.77 mmol, 42.3%) mp 305−307 °C. ^1H NMR (599.7 MHz, C_6D_6, 294 K): δ = 2.10 (s (broad), 54H, o-CH_3), 7.01 (multi, 21H). IR (cm^{-1}): The Pb−S stretching band tentatively assigned to 242.

X-ray Crystallography. Crystals **1**−**4** were removed from a Schlenk tube under N_2 and covered with a layer of hydrocarbon oil. A suitable crystal was selected, attached to a glass fiber and quickly placed in low temperature N_2 stream. The data for **1** was collected at about 90 K on a Bruker DUO APEX II CCD diffractometer with Mo

dx.doi.org/10.1021/ic302513c | Inorg. Chem. 2013, 52, 3054−3062

Table 1. Crystal Data and Structure Refinement for 1−4

compound number	1	2	3	4
empirical formula	$C_{248}H316O10Pb4$	$C_{72}H_{98}O_3PbS_2$	$C_{51.50}H_{54}Br_2Pb_2S_2$	$C_{86}H_{91}LiPbS_3$
formula weight	4285.75	1282.81	1311.26	1434.89
wavelength (Å)	0.710 73	0.710 73	0.710 73	0.710 73
crystal system	Triclinic	Monoclinic	Monoclinic	Monoclinic
space group	$P\bar{1}$	$C2/c$	$P2_1/n$	$P2_1/m$
a (Å)	16.8740(14)	24.531(4)	8.8927(8)	13.2474(5)
b (Å)	19.5017(17)	16.631(2)	40.868(4)	20.2689(7)
c (Å)	33.268(3)	16.071(2)	13.0063(12)	13.9860(5)
α (deg)	96.326(4)	90	90	90
β (deg)	92.024(5)	100.779(3)	92.323(5)	108.5190(10)
γ (deg)	91.391(5)	90	90	90
volume (Å)	10869.6(16)	6440.8(16)	4723.0(8)	3560.9(2)
Z	2	4	4	2
density (calculated) (Mg/m^3)	1.309	1.323	1.844	1.338
absorption coefficient (mm^{-1})	3.146	2.73	8.934	2.502
$F(000)$	4424	2672	2516	1.480
crystal size (mm)	0.366 × 0.265 × 0.197	0.48 × 0.33 × 0.16	0.447 × 0.434 × 0.301	0.434 × 0.271 × 0.150
crystal color and habit	pale yellow block	yellow block	colorless prism	colorless block
reflections collected	97776	7395	40295	31827
independent reflections	49485 [R(int) = 0.0221]	7395 [R(int) = 0.0000]	10796 [R(int) = 0.0294]	8385 [R(int) = 0.0182]
observed reflections ($I > 2\sigma(I)$)	42395	6398	9881	7859
data/restraints/parameters	49485/85/2479	7395/30/376	10796/2/550	8385/0/485
final R indices ($I > 2\sigma(I)$)	R1 = 0.0247	R1 = 0.0330	R1 = 0.0249	R1 =0.0217
	wR2 = 0.0567	wR2 = 0.0759	wR2 = 0.0491	wR2 = 0.0494
R indices (all data)	R1 = 0.0331	R1 =0.0418	R1 = 0.0289	R1 =0.0243
	wR2 = 0.0596	wR2= 0.0775	wR2 = 0.0500	wR2 = 0 0504

Scheme 1. Synthesis of Plumbylenes 1 and 2

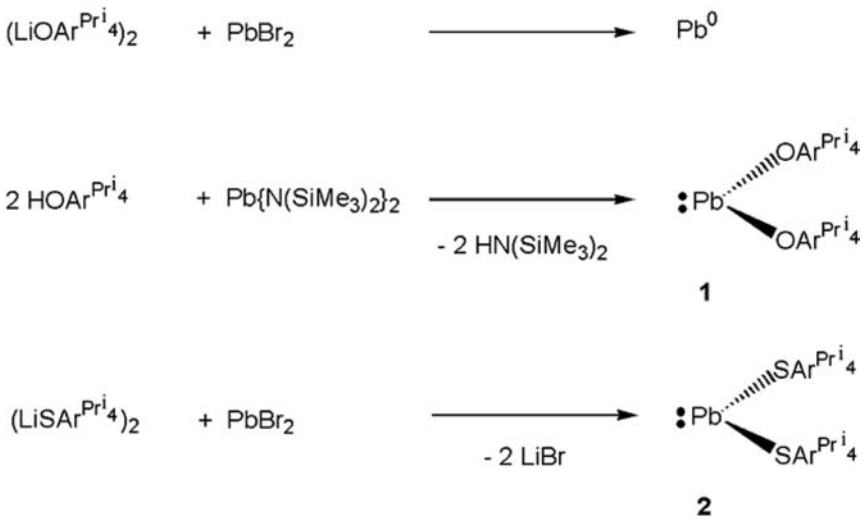

Kα (λ = 0.71073 Å) radiation. As an example, a crystal **2**, a yellow block with approximate dimensions 0.16 × 0.33 × 0.48 mm was placed and optically centered on the Bruker APEX CCD system at −183 °C (90 K).[29] Indexing of the unit cell was attempted using a random set of reflections collected from three series of 0.3° wide ω-scans, 10 s per frame, and 30 frames per series that were well distributed in reciprocal space. Four ω-scan data frame series were collected [MoKα] with 0.3° wide scans, 35 s per frame and 606, 455, 606, 455 frames collected per series at varying φ angles (φ = 0°, 90°, 180°, 270°). The crystal to detector distance was 5.23 cm, thus providing a complete sphere of data to $2\theta_{max}$ = 55.06°. The data for **3** and **4** were collected on a Bruker SMART APEX II CCD diffractometer with Mo Kα (λ = 0.71073 Å) radiation. The crystal structures (Table 1) were solved by direct methods using the SHELX version 6.1 program package.[28,29] All non-hydrogen atoms were refined anisotropically. Absorption corrections were applied using SADABS program (SADABS, an empirical absorption correction programs, part of the SAINTPlus NT version 5.0 package; Bruker AXS: Madison, WI, 1998). Thermal ellipsoid plots drawn using OLEX2 software.[30] A summary of crystal data, collection parameters, and some refinement details is given in Table 1.

RESULTS AND DISCUSSION

Synthesis. The bisthiolato plumbylene, **2**, was prepared by the addition of $(LiSAr^{Pri_4})_2$[27b] to $PbBr_2$. However, the aryloxo derivative **1** could not be prepared by this route because it led to decomposition with deposition of lead metal. Instead, an alcoholysis route involving the bisamido plumbylene, Pb{N-

dx.doi.org/10.1021/ic302513c | Inorg. Chem. 2013, 52, 3054−3062

$(SiMe_3)_2\}_2$ as the lead source, was used.[8] An overview of the synthesis of **1** and **2** is shown in Scheme 1.

The mono- and tristhiolato lead(II) complexes $\{Pb(\mu\text{-}SAr^{Me_6})Br\}_2$ (**3**) and $LiPb(\mu\text{-}SAr^{Me_6})_3$ (**4**) were prepared by the same method as **2** and isolated through multiple recrystallizations to remove the impurities as indicated by solution color. Overall, about 91.7% of the initial lead used in the reaction was accounted for in roughly equal molar amounts of **3** (43.5%) and **4** (48.4%).

The two-coordinate, V-shaped plumbylene **1** (Figure 1), was isolated as pale yellow crystals in about 56% yield and is both

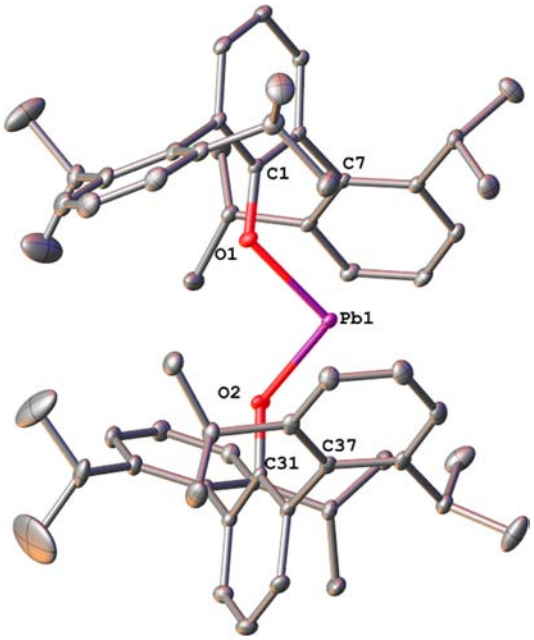

Figure 1. Thermal ellipsoid (30%) drawing of one of the crystallographically independent molecules of **1**. Hydrogen atoms and cocrystallized diethyl ether are not shown. Selected bond lengths (Å) and angles (deg): Pb(1)−O(1) 2.228(2), Pb(1)−O(2) 2.211(2), O(1)−C(1) 1.347(3), O(2)−C(31) 1.350(3), Pb(1)−C(7) 2.997(2), Pb(1)−C(37) 2.991(2), Pb(1)−Centroid(1) 2.978, Pb(1)−Centroid(2) 2.963, O(1)−Pb(1)−O(2) 100.62(6), Pb(1)−O(1)−C(1) 127.0(1), Pb(1)−O(2)−C(31) 130.1(1), O(1)−C(1)−C(2) 122.7(2), O(1)−C(1)−C(6) 119.2(2), O(2)−C(31)−C(32) 122.5(2), O(2)−C(31)−C(36) 119.2(2), Centroid(1)−Pb(1)−Centroid(2) 146.49.

thermally and photolytically stable under ambient conditions in the solid state. Nonetheless, it was found that **1** decomposes in ethereal solutions at room temperature under ambient light. The reversibly, thermochromic plumbylene becomes an intense red color upon heating and quickly returns to its original color on cooling to ambient temperature. $Pb(OAr^{Pri_4})_2$ rapidly decomposed upon melting at 295 °C. Plumbylene **2** was isolated as a microcrystalline yellow solid in about 43% yield and is thermally and photolytically stable, even in ethereal solutions. $Pb(SAr^{Pri_4})_2$ becomes orange upon heating and melts at about 211 °C.

The two crystalline products obtained from the 2:1 reaction of $LiSAr^{Me_6}$ and $PbBr_2$ were $\{Pb(\mu\text{-}SAr^{Me_6})Br\}_2$, (**3**), and $LiPb(SAr^{Me_6})_3$, (**4**). The plumbate $LiPb(\mu\text{-}SAr^{Me_6})_3$ was obtained as the first crystalline fraction as colorless blocks, in about 48% yield. These crystals were difficult to redissolve in the toluene solvent. The second crystalline fractions afforded an about 44% total yield of $\{Pb(\mu\text{-}SAr^{Me_6})Br\}_2$ (**3**). A THF solution of $\{Pb(\mu\text{-}SAr^{Me_6})Br\}_2$ has a pale yellow color at ambient temperature; however, upon warming to 65 °C the color intensifies. Cooling to ambient temperature restored the original pale yellow color. In the solid-state, heating **3** to about 246 °C, resulted in a red color which intensified until the complex melted to afford a dark red liquid at about 269 °C. Like $Pb(OAr^{Pri_4})_2$, **3** is reversibly thermochromic; however, unlike the plumbylene, **3** appears to be stable (at least temporarily) in the liquid phase.

The isolation of **3** and **4** from the reaction of 2 equiv of $LiSAr^{Me_6}$ with $PbBr_2$ contrasts with the synthesis of homoleptic **2**, which was obtained from the corresponding reaction of $LiSAr^{Pri_4}$ with $PbBr_2$. Seemingly, the reaction with $LiSAr^{Me_6}$ of any $Pb(SAr^{Me_6})_2$ produced during the synthesis of **3** and **4** is competitive with its reaction with $PbBr_2$ as $\{Pb(\mu\text{-}SAr^{Me_6})Br\}_2$. Apparently, the reaction equilibria are such that roughly equal amounts of **3** and **4** (stabilized by complexation of the Li^+ ion) are observed.

Structures. A selection of important distances and angles for **1**−**4** is given in Table 2.

A single crystal X-ray diffraction study shows that **1** crystallizes with four monomeric molecules and two solvent ethers in the asymmetric unit with an average Pb···Pb separation of 10.920(1) Å. The average O−Pb−O and Pb−O−C angles are 99(1)° and 127(2)°. The O−Pb−O angle is significantly wider than that reported for $Pb(BHT)_2$ (86.2(4)°) whereas the Pb−O−C angle is similar to the 124(2)° in $Pb(BHT)_2$.[10] The average Pb−O bond length is 2.216(8) Å which is at the upper end of the known range (2.17(1)−2.240(5) Å) for Pb(II)−O bond lengths found in aggregated complexes of formulas $\{Pb(OR)_2\}_n$.[31−34] Using the molecule containing Pb(1) as a representative example, the closest approach between other ligand-atoms and lead involves Pb(1)−C(37) (2.991(2) Å), and the Pb−centroid distance is 3.38(4) Å—both of which are within the sum of Pb−C van der Waals radii (3.72 Å)[35] but more than 0.7 Å longer than a typical Pb(II)−C distance of 2.19 Å.[36]

The plumbylene **2** (Figure 2) crystallizes as a two-coordinate, V-shaped monomer with a crystallographically required 2-fold

Table 2. Selected Distances (Å) and Angles (deg) for Pb(II) Chalcogenolate Complexes $(Pb(ChAr)_2)$, Ch = O (1), S (2); $\{Pb(\mu\text{-}SAr^{Me_6})Br\}_2$ (3) [Pb(1) and Pb(2) sites], and $LiPb(\mu\text{-}SAr^{Me_6})_3$ (4)

compound	Pb−Ch	Ch−Pb−Ch	Pb−Ch−C	Pb−Ch−C−C	Ch−C	Pb−Centroid	Ch···Ch
(1) $Pb(OAr^{Pri_4})_2$	2.216(8)[a]	99(1)[a]	127(2)[a]	26(5)[a]	1.35(2)[a]	2.95(3)[a]	3.38(4)[a]
(2) $Pb(SAr^{Pri_4})_2$	2.5656(9)	77.21(4)	113.42(11)	31.0(1)	1.771(3)	3.046	3.202(1)
(3) $\{Pb(\mu\text{-}SAr^{Me_6})Br\}_2$[Pb(1)]	2.806(3)[a]	74.46(2)	113.5(3)[a]	34(10)[a]	1.784(1)[a]	3.2(3)[a]	3.396(1)
(3) $\{Pb(\mu\text{-}SAr^{Me_6})Br\}_2$[Pb(2)]	2.727(3)[a]	77.02(3)	110.9(3)[a]	50(11)[a]	1.784(1)[a]	3.5(3)[a]	3.396(1)
(4) $LiPb(\mu\text{-}SAr^{Me_6})_3$	2.675(4)[a]	81.1(5)[a]	118.9(5)[a]	42.8(3)[a]	1.780(1)[a]	3.702(9)[a]	3.1(5)[a]

[a]Average value.

dx.doi.org/10.1021/ic302513c | Inorg. Chem. 2013, 52, 3054−3062

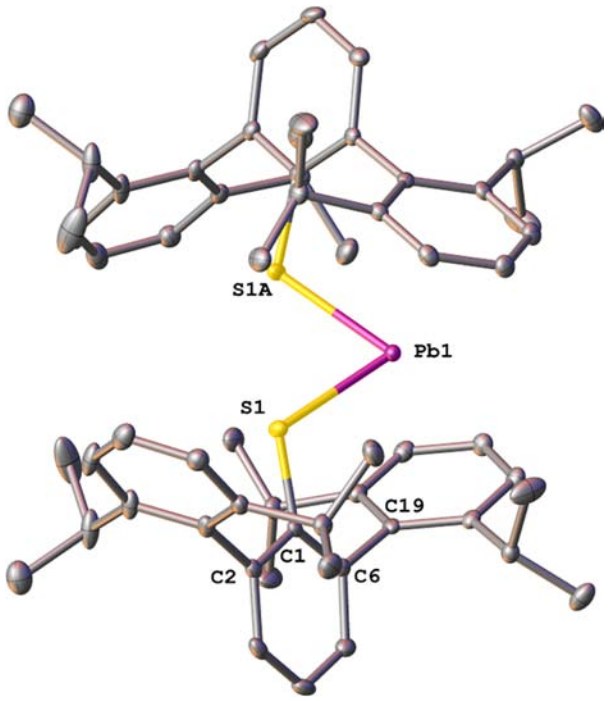

Figure 2. Thermal ellipsoid (30%) drawing of **2**. Hydrogen atoms and two cocrystallized THF molecules are not shown. Selected bond lengths (Å) and angles (deg): Pb(1)−S(1) 2.5656(9), S(1)−C(1) 1.771(3), Pb(1)···C(19) 3.170(3), Pb(1)···Centroid 3.046, S(1)−Pb(1)−S(1A) 77.21(4), Pb(1)−S(1)−C(1) 113.42(11), S(1)−C(1)−C(2) 116.0(3), S(1)−C(1)−C(6) 123.8(2), Centroid−Pb(1)−Centroid 144.21.

axis and 9.5139(9) Å intermolecular Pb···Pb separation. It has an acute S−Pb−S interligand angle of 77.21(4)° which can be compared to the angles in cyclic dimers and trimers (73.5(1)−92.8(1)°)[9,12,14] or in the Lewis base complexed monomer, $Pb(SR_f)_2(THF)$ (R_f = C_6H_2-2,4,6-$(CF_3)_3$) (84.4(1)°);[37] although it is wider than some angles in polymeric, base stabilized species such as $\{Pb(SPh)_2(Py)\}_n$ (70.05(5)°).[38] The Pb−S bond length is 2.5656(9) Å which is near the shorter end of the 2.554(5)−2.981(1) Å range observed in the aggregated and base stabilized lead(II) thiolates mentioned above.[9,14,38,39] It should be noted that the Pb−S length in the plumbylene, Pb(Tbt)(STbt) (2.498(10) Å), is distinctly shorter than that in **2**.[13] The difference could be a result of decreased interligand steric repulsion within Pb(Tbt)(STbt). The Pb−S−C angle is 113.42(11)° with C−S distances of 1.771(3) Å which is wider than the Pb−S−C angle (107.4(6)°) and shorter than the C−S distance (1.88(1) Å) found in Pb(Tbt)(STbt).[13] The closest nonbonded ligand approach to lead involves C(19) at 3.170(3) Å which is within the sum of Pb−C van der Waals radii (3.72 Å).[35] The closest approach between Pb(1) and a THF oxygen is 5.420(7) Å and is well above the sum of the Pb−O van der Waals radii (3.54 Å).[35]

The S−Pb−S angle in **2** is about 22° narrower than the corresponding O−Pb−O angle in **1**. One of the reasons for the difference in the angles may be the shorter Pb−O bonds[36] and greater EN character of the OAr^{Pri_4} ligand which afford greater bond pair-bond pair repulsions and produce a less diffuse metal lone pair leading to the wider angle in **1**.[3] However, such a large disparity in the interligand angle is not observed between $Sn(BHT)_2$ (O−Sn−O = 88.8(2)°),[8] $Sn(OC_6H_3$-2,6-$Bu^t_2)_2$, (O−Sn−O = 88.8(1)°),[40] and $Sn(SMes^*)_2$ (S−Sn−S = 85.4(1)°)[9] which are the only closely related pairs of divalent group 14 element aryloxide and thiolates for which data are available. Thus, it seems probable that the acute S−Pb−S angle of **2** may result from the peculiar steric characteristics of the terphenyl substituent which produce both front side (side of the lead lone pair) and back side (the side of the sulfurs) interactions that involve a combination of imperfectly understood steric, dispersion, and packing forces that afford the unusual angles.[41] Geminal bonding interactions between the two Pb−S bonds are also plausible,[42] suggesting that the complex is effectively an intermediate "snapshot" of disulfide elimination.[43]

The monothiolato lead(II) bromide complex **3**, (Figure 3) crystallizes as a thiolate bridged dimer featuring an asymmetric, puckered, four-membered Pb_2S_2 ring core. The structure may be contrasted with those of the centrosymmetric, aryl lead(II)

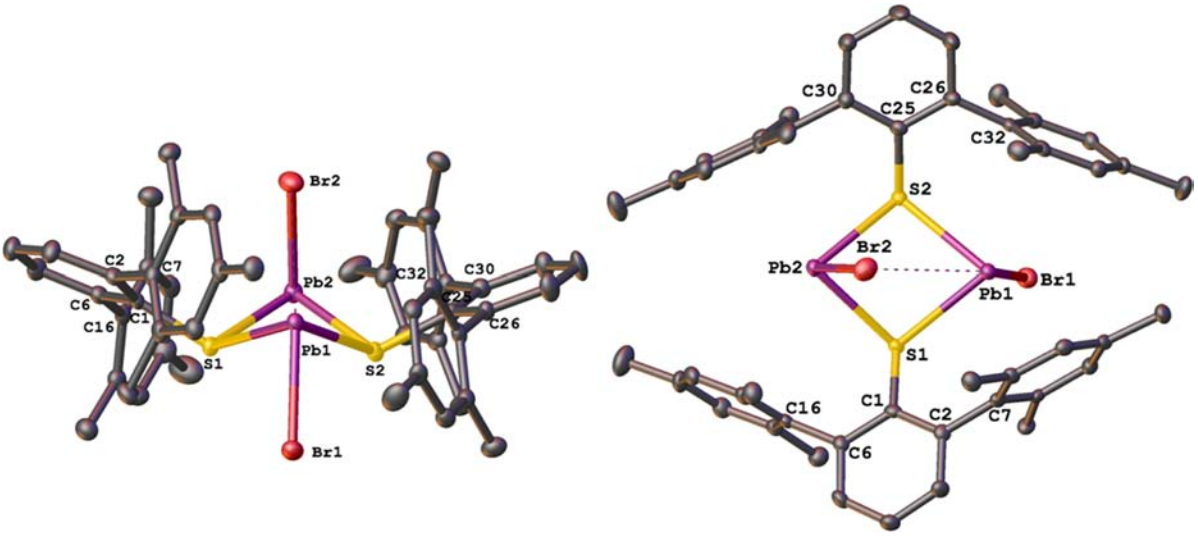

Figure 3. Thermal ellipsoid (30%) drawings of **3**. Hydrogen atoms and one molecule of cocrystallized toluene are not shown for clarity. Selected bond lengths (Å) and angles (deg): Pb(1)−S(1) 2.8096(9), Pb(1)−S(2) 2.8029(9), Pb(1)−Br(1) 2.693(1), Pb(1)···Br(2) 3.792(1), Pb(2)−S(1) 2.7299(9), Pb(2)−S(2) 2.7239(9), S(1)−Pb(1)−S(2) 74.46(2), Pb(2)−Br(2) 2.7108(5), S(1)−Pb(2)−S(2) 77.02(3).

dx.doi.org/10.1021/ic302513c | Inorg. Chem. 2013, 52, 3054−3062

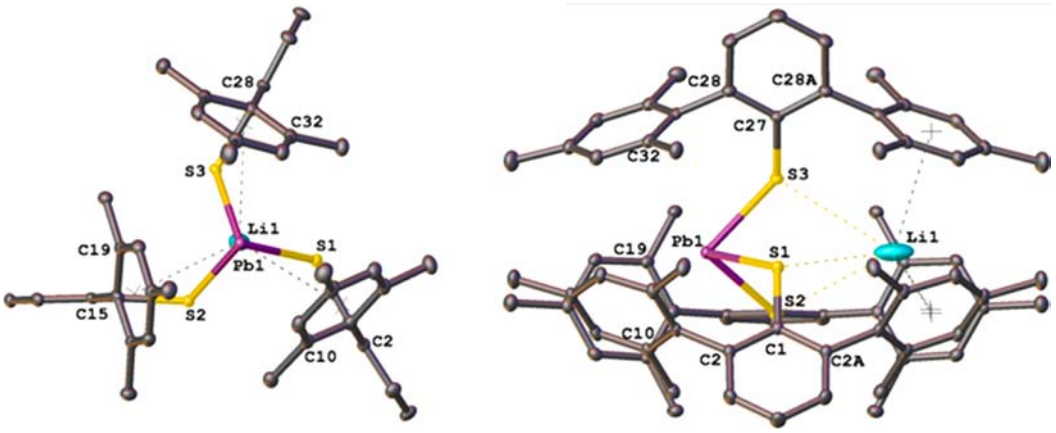

Figure 4. Thermal ellipsoid (30%) drawing of **4**. Hydrogen atoms are not shown. Selected bond lengths (Å) and angles (deg): Pb–S(1) 2.6783(4), Pb–S(2) 2.6781(4), Pb–S(3) 2.6693(4), S(1)–Pb–S(2) 80.46(1), S(1)–Pb–S(3) 81.56(1), and S(2)–Pb–S(3) 80.38(1).

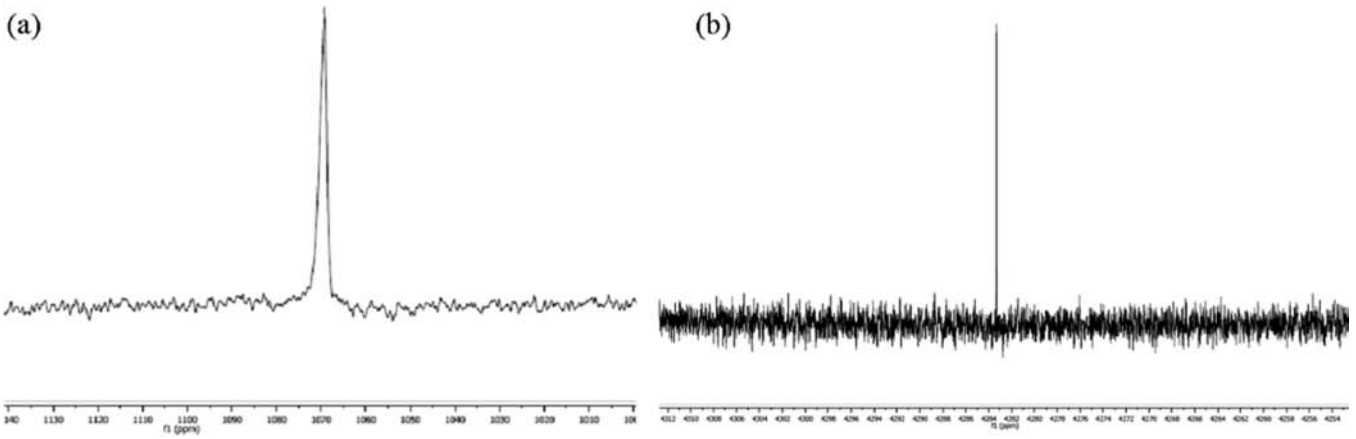

Figure 5. ^{207}Pb NMR spectra of (a) $Pb(OAr^{Pri_4})_2$ (**1**) and (b) $Pb(SAr^{Pri_4})_2$ (**2**).

halide dimers $(Ar^{Pri_4}PbBr)_2$ and $(Ar^{Pri_6}PbBr)_2$ which are associated through halogen bridging.[44,45] The intramolecular Pb···Pb distance is 4.0011(9) Å and the closest intermolecular Pb···Pb distance is 10.144(1) Å. Pb(1) features a distorted saw-horse geometry with a stereochemically active lone pair directed perpendicular to the planes of the central arenes of the terphenyl ligands.[23] The Pb(1) atom is bonded to two bridging sulfur atoms, and to Br(1) which is *exo* to the Pb_2S_2 ring. It also possesses a long interaction to Br(2) (3.792(1) Å) that is *endo* to the Pb_2S_2 moiety (cf. sum of the van der Waals radii for Pb–Br = 3.87 Å).[35] The bridging Pb(1)–S(1) and Pb(1)–S(2) distances, 2.8096(9) and 2.8029(9) Å, are significantly longer (ca. 0.25 Å) than the Pb–S distance observed in **2**, although they are within the range of distances discussed for aggregated bisthiolato lead complexes.[9,14,38,39] The Pb(1)–Br(1) distance, 2.693(1) Å, is shorter than those in of $(Ar^{Pri_4}PbBr)_2$ and $(Ar^{Pri_6}PbBr)_2$ which have average Pb–Br distances of about 2.92 Å.[44,45] The S(1)–Pb(1)–S(2) angle of 74.46(2)° is slightly narrower than the S–Pb–S angle in **2** (77.21(4)°) but is similar to angles observed for the central, tetra-coordinate lead atom in $\{Pb(SC_6H_3\text{-}2,6\text{-}Pr^i_2)_2\}_3$ (73.5(1)°).[9] The distances between Pb(1) and the centroids of the two closest arene rings are 2.984 and 3.494 Å while the centroid–Pb(1)–centroid angle is 116.87°. The Pb(2) atom has similar Pb(2)–S(1) and Pb(2)–S(2) distances of 2.7299(9) and 2.7239(9) Å as well as a S–Pb(2)–S angle of 77.02(3)°. The Pb(2)–Br(2) distance, 2.7108(5) Å, is slightly elongated (by ca. 0.02 Å) in comparison to Pb(1)–Br(1), perhaps as a result of Br(2)···Pb(1) interaction. The distances between Pb(2) and the centroids of the two closest arene rings are 3.715 and 3.200 Å, respectively, and the centroid–Pb(2)–centroid angle is 112.00°. Thus, the structural data show that the distances to Pb(1) are about 0.1 Å longer then the Pb–S distances to Pb(2). The longer distances arise from the higher effective coordination number of Pb(1) due to its interaction with Br(2) in addition to Br(1), S(1), and S(2).

The lithium trithioplumbate **4** (Figure 4) crystallizes as monomeric units with a trigonal pyramidal geometry at lead and about 10.4307(3) Å intermolecular Pb···Pb separations. The lithium and lead atoms are disordered over two sites. The Li–S distances, (Li–S(1) 3.584(16) Å, Li–S(2) 3.560(16) Å, and Li–S(3) 3.539(15) Å), are much longer than the range of Li–S distances (2.33(2)–2.65(2) Å) in the precursor, $LiSAr^{Me_6}$, which is a trimer in the solid state, wherein the lithiums interact with two thiolato sulfurs.[26,46] The lithium ions also display contacts to the centroids of the flanking mesityl substituents with Li–centroid distances of 3.23(1), 3.56(2), and 3.18(1) to the C(5), C(18), and C(31) rings, such that the Li^+ ion is encapsulated in a cavity composed of the thiolate sulfurs and flanking mesityls. The Pb–S bond lengths are 2.6783(4), 2.6781(4), and 2.6693(4) Å and are longer than those in Payne's complex, $[As(C_6H_5)_4][Pb(SPh)_3]$ which has Pb–S bond lengths of 2.619(1), 2.623(1), and 2.647(1) Å, but are similar to those in $[NPr^n_4][Pb(SPh)_3]$[25] which was prepared by

dx.doi.org/10.1021/ic302513c | *Inorg. Chem.* 2013, 52, 3054–3062

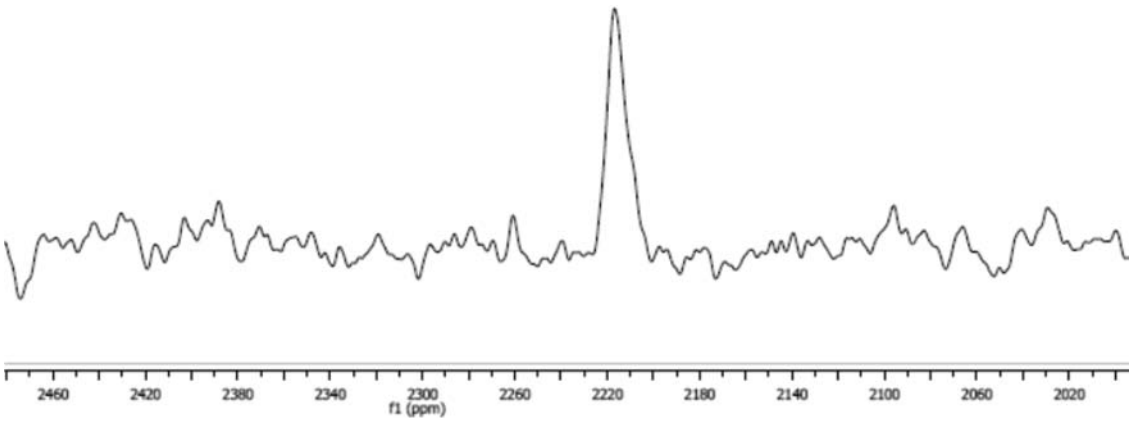

Figure 6. ^{207}Pb NMR spectrum of $\{PbBr(\mu\text{-}SAr^{Me_6})\}_2$ (**3**).

Christou and co-workers and has Pb−S distances of 2.696(3), 2.665(3), and 2.633(3) Å. The S−Pb−S angles of **4** are 80.46(1), 81.56(1), and 80.38(1)° and are about 10° narrower than those in the Payne (90.32(4)°, 91.08(5)°, 96.14(5)°) and Christou (89.7(1)°, 93.7(1)°, 102.7(1)°) complexes. The Pb−S−C angles of **4** are 119.40(5), 118.34(4), and 118.95(5)° and are considerably wider than the Pb−S−C angles in complexes of Payne (101.4(1), 98.8(2), and 97.1(2)°) and Christou (98.1(3), 94.9(3), and 93.7(3)°). The distances between lead and the centroids of the three closest arene rings are 3.703, 3.690, and 3.713 Å which are just within the sum of the van der Waals radii for lead and carbon (Pb−C = 3.72 Å).[35] The closest other atoms to lead are the *ortho*-carbons, of the flanking arene rings (C(6), C(19, and C(32)) that have Pb−C distances of 3.402(2), 3.414(1), and 3.373(2) Å. A list of selected distances and angles for compounds **1**−**4** are given in Table 2.

Spectroscopic Analysis. The ^{207}Pb NMR signal for **1** was identified at δ = 1070.3 (Figure 5a). For **2**, the ^{207}Pb NMR signal appears significantly further downfield at δ = 4283.2 (Figure 5b). Thus, the chemical shifts of the signals of **1** and **2** are the opposite of what is expected on the basis of the σ-inductive effects of oxygen and sulfur. The difference is likely due to greater contributions from the paramagnetic term, σ_p, in **2** where the energy separation between the highest occupied molecular orbital (HOMO) and the lowest unoccupied molecular orbital (LUMO) is less than that of **1** (see below).[47] This results in a deshielding of the nucleus and consequently a more downfield chemical shift than that in **1**.[47] Both signals are well upfield of that observed or the diaryl plumbylene, $Pb(Ar^{Pri_4})_2$, which has a ^{207}Pb NMR chemical shift of δ = 9430.[48,49] The downfield shift of the diaryl plumbylenes bearing the more electropositive substituents is consistent with greater paramagnetic interactions involving the excited state which acts to deshield the ^{207}Pb NMR nucleus.[1a,48−50] The shift of **2** is comparable to bisamido plumbylenes such as $Pb\{N(SiMe_3)_2\}_2$ (δ = 4916).[50] However, it contrasts with the chemical shift observed for the previously reported bis-(terphenyl)amido plumbylene, $Pb(\{N(H)Ar^{Me_6}\}_2$, (Ar^{Me_6} = C_6H_3-2,6-(C_6H_2-2,4,6- $Me_3)_2$) (δ = 2871) which probably has Pb···C interactions with the terphenyl substituents.[51] The ^{207}Pb NMR signal for **2** is significantly further downfield than the monomeric and dimeric, three- and four-coordinate pyridine adducts of lead dithiolates (δ = 2733−2873) reported by Briand et al.[52]

The ^{207}Pb NMR signal for **3** (Figure 6) is broad ($\nu_{1/2}$ = 351 Hz) with a chemical shift of δ = 2223. This is significantly upfield of **2** as well as the range of three-coordinate lead(II) thiolates observed by Briand and Dean (δ = 2518−2999);[52,53] though, it is downfield of **1**. The most probable explanation may arise from the fact that bromine is more electronegative (2.96) than sulfur (2.58), which also stabilizes the lone-pair orbitals on the lead atoms. The broadness of the signal may be due to an equilibrium between the two lead sites as it has been shown that line broadening can occur when multiple lead sites rapidly exchange ligands.[53] Possibilities include an equilibrium between the trigonal pyramidal and saw-horse geometries, which sees the bromines alternate between the *endo* and *exo* positions, or a simple equilibrium where the site of dimer bridging alternates between the thiolates and the bromides.

Although no structure of alkali metal complexed trithiolato plumbates such as **4** have been previously determined, ^{207}Pb NMR studies have shown that excess LiSPh can react with polymeric $[Pb(SPh)_2]_n$ to give a lithium trithioplumbate complex that possesses a labile thiolate ligand and produces chemical shifts in the region of δ = 2518−2999.[52,53] Despite this information, several attempts to acquire a signal for **4** proved fruitless. It is unclear if this is due to the low solubility of **4** or other effects associated with solvent or temperature.[53]

In the electronic spectra, the most noticeable difference between the plumbylenes is a red shift of the two lowest energy absorptions between **1** to **2**. Based on data for other plumbylenes, the lowest energy transition likely originates from a lead 6n → 6p transition for both **1** (370 nm) and **2** (422 nm).[1,54] The higher transition energy of **1** is likely due to electron-withdrawing effects from the more electronegative oxygen which stabilizes the lead lone pair.[54,55] The amount of π-bonding from the chalcogen lone-pair to the lead p orbital is most likely small as it was recently shown that a silicon complex, $Si(SAr^{Me_6})_2$, related to $Pb(SAr^{Pri_4})_2$ has only a minor degree of Si−S π-bonding.[56] In the absence of data for a series of compounds, it is unclear how much the Ch−Pb−Ch angle affects the energy of the HOMO−LUMO gap as well as other transitions.

CONCLUSIONS

Two isolobal examples of monomeric, two-coordinate dichalcogenolate plumbylenes have been isolated and fully characterized. The structural data reveal a large disparity in the Ch−Pb−Ch bond angle with the dithiolate plumbylene being about 22° narrower. In addition, it has been demonstrated that the steric congestion of the aryl group can greatly affect the metathesis reaction pathway as attempts to produce the less

dx.doi.org/10.1021/ic302513c | *Inorg. Chem.* 2013, 52, 3054−3062

hindered bisthiolato plumbylene, $Pb(SAr^{Me_6})_2$, by the same method as **2** resulted in the synthesis of both the mono- and trithiolato lead(II) complexes **3** and **4**. As a whole, complexes **1**–**4** demonstrate that the steric loading at the lead(II) ion can have dramatic consequences on the geometry. Furthermore, these results suggest that steric effects should be strongly considered when attempting to understand how lead and other heavy metals distort the geometry of metalloenzymes, since it has been shown the electronic factors only account for part of the story. Future work will investigate the effects that govern the contraction of the Ch–M–Ch bond angle and its possible origin in dispersion forces between the bulky terphenyl substituents.

■ ASSOCIATED CONTENT

Ⓢ Supporting Information

^{1}H NMR spectra of **1** and **2**, CIF files, and further thermal ellipsoid plots for the X-ray structures of **1**, **2**, **3**, and **4**. Expanded table of bond lengths and angles for the structures of **1**, **2**, **3**, and **4**. This material is available free of charge via the Internet at http://pubs.acs.org.

■ AUTHOR INFORMATION

Corresponding Author

*E-mail: power@chem.ucdavis.edu.

Present Address

†Department of Chemistry, University of Nevada, Reno, 1664 N Virginia St., Reno, NV 89512.

Author Contributions

The manuscript was written through contributions of all authors.

Notes

The authors declare no competing financial interest.

■ ACKNOWLEDGMENTS

We are grateful to the U.S. National Science Foundation for research funding (Grant CHE-09848417) and for the dual source X-ray diffractometer (Grant 0840444).

■ REFERENCES

(1) (a) Lee, V. Y.; Sekiguchi. A. *Organometallic Compounds of Low-Coordinate Si, Ge, Sn and Pb: From Phantom Species to Stable Compounds*; John Wiley & Sons Ltd: Chichester, U.K., 2010; pp 139–188. (b) Mizuhata, Y.; Sasamori, S.; Tokitoh, N. *Chem. Rev.* **2009**, *109*, 3479–3511. (c) Tokitoh, N.; Ando, W. *Reactive Intermediate Chemistry*; Moss, R. A., Platz, M. S., Jones, M., Jr., Eds.; Wiley: Hoboken, NJ, 2004; Chapter 14. (d) Asay, M.; Jones, C.; Driess, M. *Chem. Rev.* **2011**, *111*, 354–396. (e) Zabula, A. V.; Hahn, F. E. *Eur. J. Inorg. Chem.* **2008**, 5165–5179.

(2) (a) Drago, R. S. *J. Phys. Chem.* **1958**, *62*, 353–357. (b) Pyykkö, P. *Chem. Rev.* **1988**, *88*, 563–594. (c) Shimoni-Livny, L.; Glusker, J. P.; Bock, C. W. *Inorg. Chem.* **1998**, *37*, 1853–1867.

(3) Weidenbruch, M. *Organometallics* **2003**, *22*, 4348–4360.

(4) (a) Davidson, D. J.; Lappert, M. F. *J. Chem. Soc., Chem. Commun.* **1973**, 317. For recent work on the related N-heterocyclic plumbylenes, see: (b) Hahn, E. F.; Heitmann, D.; Pape, T. *Eur. J. Inorg. Chem.* **2008**, 1039–1041. (c) Charmant, J. P. H.; Haddow, M. F.; Hahn, F. E.; Heitmann, D.; Fröhlich, R.; Mansell, S. M.; Russell, C. A.; Wass, D. F. *Dalton. Trans.* **2008**, 6055–6058. (d) Refs 1d and 1e.

(5) (a) Stürmann, M.; Weidenbruch, M.; Klinkhammer, K. W.; Lissner, F.; Marsmann, H. *Organometallics* **1998**, *17*, 4425–4428. (b) Klinkhammer, K. W. In *Chemistry of Organic Germanium, Tin and Lead Compounds*; Rappoport, Z., Ed.; Wiley: New York, 2002; Vol. 2, pp 283–357.

(6) Harris, D. H.; Lappert, M. F. *J. Chem. Soc., Chem Commun.* **1974**, 895.

(7) Fjeldberg, T.; Hope, H.; Lappert, M. F.; Power, P. P.; Thorne, A. J. *J. Chem. Soc., Chem. Commun.* **1983**, 639–641.

(8) Cetinkaya, B.; Gümrükcü, I.; Lappert, M. F.; Atwood, J. L.; Rogers, R. D.; Zaworotko, M. J. *J. Am. Chem. Soc.* **1980**, *102*, 2088–2089.

(9) Hitchcock, P. B.; Lappert, M. F.; Samways, B. J.; Weinberg, E. L. *J. Chem. Soc., Chem. Commun.* **1983**, 1492–1494.

(10) Lappert, M. F. *Main Group Met. Chem.* **1994**, *17*, 183–207.

(11) Hitchcock, P. B.; Jasim, H. A.; Kelly, R. E.; Lappert, M. F. *J. Chem. Soc., Chem. Commun.* **1985**, 1776–1778.

(12) Wojnowski, W.; Wojnowski, M.; Peters, K.; Peters, E.-M.; Schnering, H. G. *Z. Anorg. Allg. Chem.* **1986**, *535*, 56–62.

(13) (a) Kano, N.; Tokitoh, N.; Okazaki, R. *Organometallics* **1997**, *16*, 4237–4239. (b) Tokitoh, N.; Kano, N.; Okazaki, R. *Phosphorus, Sulfur Silicon Relat. Elem.* **1999**, *153*, 333–334.

(14) Davidovich, R. L.; Stavila, V.; Whitmire, K. H. *Coord. Chem. Rev.* **2010**, *254*, 2193–2226.

(15) (a) Machol, J. L.; Wise, F. W.; Patel, R. C.; Tanner, D. B. *Phys. Rev. B.* **1993**, *48*, 2819–2822. (b) Dutta, A. K.; Ho, T.; Zhang, L.; Stroeve, P. *Chem. Mater.* **2000**, *12*, 1042–1048.

(16) (a) Noheda, B. *Curr. Opin. Solid State Mater. Sci.* **2002**, *6*, 27–34 , and references contained within. (b) Turova, N. Y.; Turevskaya, E. P.; Kessler, V. G.; Yanovskaya, M. I. *The Chemistry of Metal Alkoxides*; Kluwer Academic Publishers: Norwell, MA, 2002; pp 141–144.

(17) Yao, S.; Block, S.; Brym, M.; Driess, M. *Chem. Commun.* **2007**, 3844–2846.

(18) Tam, E. C. Y.; Johnstone, N. C.; Ferro, L.; Hitchcock, P. B.; Fulton, J. R. *Inorg. Chem.* **2009**, *48*, 8971–8976.

(19) Magyar, J. S.; Weng, T. -C.; Stern, C. M.; Dye, D. F.; Rous, B. W.; Payne, J. C.; Bridgewater, B. M.; Mijovilovich, A.; Parkin, G.; Zaleski, J. M.; Penner-Hahn, J. E.; Godwin, H. A. *J. Am. Chem. Soc.* **2005**, *127*, 9495–9505 , and references therein.

(20) (a) Warren, M. J.; Cooper, J. B.; Wood, S. P.; Shoolingin-Jordan, P. M. *Trends. Biochem. Sci.* **1998**, *23*, 217–221. (b) Godwin, H. A. *Curr. Opin. Chem. Biol.* **2001**, *5*, 223–227.

(21) (a) Erskine, P. T.; Senior, N.; Awan, S.; Lambert, R.; Lewis, G.; Tickle, I. J.; Sarwar, M.; Spencer, P.; Thomas, P.; Warren, M. J.; Shoolingin-Jordan, P. M.; Wood, S. P.; Cooper, J. B. *Nat. Struct. Biol.* **1997**, *4*, 1025–1031. (b) Erskine, P. T.; Norton, E.; Cooper, J. B.; Lambert, R.; Coker, A.; Lewis, G.; Spencer, P.; Sarwar, M.; Wood, S. P.; Warren, M. J.; Shoolingin-Jordan, P. M. *Biochemistry* **1999**, *38*, 4266–4276. (c) Jaffe, E. K.; Martins, J.; Li, J.; Kervinen, J.; Dunbrack, R. L., Jr. *J. Biol. Chem.* **2001**, *276*, 1531–1537.

(22) Bridgewater, B. M.; Parkin, G. *J. Am. Chem. Soc.* **2000**, *122*, 7140–7141.

(23) Jarzecki, A. A. *Inorg. Chem.* **2007**, *46*, 7509–7521.

(24) Dean, P. A. W.; Vittal, J. J.; Payne, N. C. *Inorg. Chem.* **1984**, *23*, 4232–4236.

(25) Christou, G.; Folting, K.; Huffman, J. C. *Polyhedron.* **1984**, *3*, 1247–1253.

(26) Ellison, J. J.; Ruhlandt-Senge, K.; Power, P. P. *Angew. Chem., Int. Ed. Engl.* **1994**, *33*, 1178–1180.

(27) (a) Stanciu, C.; Olmstead, M. M.; Phillips, A. D.; Stender, M.; Power, P. P. *Eur. J. Inorg. Chem.* **2003**, 3495–3500. (b) Sutton, A. D.; Fettinger, J. C.; Rekken, B. D.; Power, P. P. *Polyhedron* **2008**, *27*, 2337–2340.

(28) Sheldrick, G. M. *SHELXTL*, Version 6.1; Siemens Analytical X-ray Instruments Inc.: Madison, WI, 2002.

(29) Sheldrick, G. M. *SHELXS97 and SHELXL97*; Universität Göttingen: Göttingen, Germany, 1997.

(30) Dolomanov, O. V.; Bourhis, L. J.; Gildea, R. J.; Howard, J. A. K.; Puschmann, H. *J. Appl. Crystallogr.* **2009**, *42*, 339–341.

(31) Papiernik, R.; Hubert-Pfalzgraf, L .G.; Massiani, M. C. *Inorg. Chim. Acta. Lett.* **1989**, *165*, 1–2.

(32) (a) Goel, S. C.; Chiang, M. Y.; Buhro, W. E. *Inorg. Chem.* **1990**, *29*, 4640–4646. (b) Papiernik, R.; Hubert-Pfalzgraf, L. G.; Massiani, M. C. *Polyhedron* **1991**, *10*, 1657–1662. (c) Suh, S.; Hoffman, D. M.

Inorg. Chem. **1996**, *35*, 6164−6169. (d) Mehrotra, R. C.; Rai, A. K.; Jain, A. *Polyhedron* **1991**, *10*, 1103−1104.
(33) Van Zandt, W.; Huffman, J. C.; Stewart, J. L. *Main Group Met. Chem.* **1998**, *21*, 237−240.
(34) Barrau, J.; Rima, G.; El Amaraoui, T. *Organometallics* **1998**, *17*, 607−614.
(35) (a) Bondi, A. *J. Phys. Chem.* **1964**, *68*, 441−452. (b) Rowland, R. S.; Taylor, R. *J. Phys. Chem.* **1996**, *100*, 7384−7391.
(36) Pyykkö, P.; Matsumi, S. *Chem.—Eur. J.* **2009**, *15*, 186−197.
(37) Labahn, D.; Brooker, S.; Sheldrick, G. M.; Roesky, H. W. *Z. Anorg. Allg. Chem.* **1992**, *610*, 163−168.
(38) Appleton, S. E.; Briand, G. G.; Decken, A.; Smith, A. S. *Dalton Trans.* **2004**, 3515−3520.
(39) Briand, G. G.; Decken, A.; Finniss, M. C.; Gordon, A. D.; Hughes, N. E.; Scott, L. M. *Polyhedron* **2012**, *33*, 171−178.
(40) Barnhart, D. M.; Clark, D. L.; Watkin, J. G. *Acta. Crystallogr., Sect. C: Cryst. Struct. Commun.* **1994**, *50*, 702−204.
(41) (a) Ndambuki, S.; Ziegler, T. *Inorg. Chem.* **2012**, *51*, 7794−7800. (b) Heitmann, D.; Paper, T.; Hepp, A.; Mück-Lichtenfeld, C.; Grimme, S.; Hahn, F. E. *J. Am. Chem. Soc.* **2011**, *133*, 11118−11120.
(42) Naruse, Y.; Inagaki, S. *Top. Curr. Chem.* **2009**, *289*, 265−291.
(43) (a) Berthon-Gelloz, G.; de Bruin, B.; Tinant, B.; Markó, I. E. *Angew. Chem., Int. Ed.* **2009**, *48*, 3161−3164. (b) Takagi, N.; Sakaki, S. *J. Am. Chem. Soc.* **2012**, *134*, 11749−11759.
(44) Pu, L.; Twamley, B.; Power, P. P. *Organometallics* **2000**, *19*, 2874.
(45) Hino, S.; Olmstead, M. M.; Phillips, A. D.; Wright, R. J.; Power, P. P. *Inorg. Chem.* **2004**, *43*, 7346.
(46) Niemeyer, M.; Power, P. P. *Inorg. Chem.* **1996**, *35*, 7264−7272.
(47) (a) Ramsey, N. F. *Phys. Rev.* **1950**, *78*, 699−703. (b) Müller, T. *J. Organomet. Chem.* **2003**, *686*, 251−256.
(48) Spikes, G. H.; Peng, Y.; Fettinger, J. C.; Power, P. P. *Z. Anorg. Allg. Chem.* **2006**, *632*, 1005−1010.
(49) The range of chemical shifts of the ^{207}Pb NMR signals for diaryl and dialkyl plumbylenes is about δ = 5000−11000, see refs 1 and 50.
(50) Wrackmeyer, B. *Annu. Rep. NMR Spectrosc.* **2002**, *47*, 1−37.
(51) Merrill, W. A.; Wright, R. J.; Stanciu, C. S.; Olmstead, M. M.; Fettinger, J. C.; Power, P. P. *Inorg. Chem.* **2010**, *49*, 7097−7105.
(52) Briand, G. G.; Smith, A. D.; Schatte, G.; Rossini, A. J.; Schurko, R. W. *Inorg. Chem.* **2007**, *46*, 8625−8637.
(53) Arsenault, J. J. I.; Dean, P .A. W. *Can. J. Chem.* **1983**, *61*, 1516−1523.
(54) Electronic spectra for tetrylenes, see: (a) Apeloig, Y.; Karni, M.; West, R.; Welsh, K. *J. Am. Chem. Soc.* **1994**, *116*, 9719. (b) Apeloig, Y.; Karni, M. *J. Chem. Soc., Chem. Commun.* **1985**, 1048. (c) Michalczyk, M. J.; Fink, M. J.; DeYoung, D. J.; Carlson, C. W.; Welsh, K. M.; West, R.; Michl, J. *Silicon, Germanium, Tin Lead Compd.* **1986**, *9*, 75.
(55) (a) Magnusson, E. *J. Am. Chem. Soc.* **1984**, *106*, 1177−1185. (b) Magnusson, E. *J. Am. Chem. Soc.* **1984**, *106*, 1185−1191.
(56) Rekken, B. D.; Brown, T. M.; Fettinger, J. C.; Tuononen, H. M.; Power, P. P. *J. Am. Chem. Soc.* **2012**, *134*, 6504−6507.